A ZnO nanowire resistive switch

K. R. G. Karthik, Rajiv Ramanujam Prabhakar, L. Hai, Sudip K. Batabyal, Y. Z. Huang, and S. G. Mhaisalkar

Citation: Applied Physics Letters **103**, 123114 (2013); doi: 10.1063/1.4821994
View online: http://dx.doi.org/10.1063/1.4821994
View Table of Contents: http://scitation.aip.org/content/aip/journal/apl/103/12?ver=pdfcov
Published by the AIP Publishing

A ZnO nanowire resistive switch

K. R. G. Karthik,[1,2] Rajiv Ramanujam Prabhakar,[3] L. Hai,[1] Sudip K. Batabyal,[3] Y. Z. Huang,[1,a)] and S. G. Mhaisalkar[1,2,3]

[1]*School of Materials Science and Engineering, Nanyang Technological University, 50 Nanyang Avenue, Singapore 639798*
[2]*TUM CREATE Centre for Electromobility, 62 Nanyang Drive, Block N1.2, Singapore 637459*
[3]*Energy Research Institute @NTU (ERI@N), Nanyang Technological University, Research Techno Plaza, 5th Storey, 50 Nanyang Drive, Singapore 637553*

(Received 3 June 2013; accepted 1 September 2013; published online 20 September 2013)

An individual ZnO nanowire resistive switch is evaluated with Pt/ZnO nanowire/Pt topology. A detailed DC I-V curve analysis is performed to bring both the conduction mechanism and the device characteristics to light. The device is further studied at various vacuum pressures to ascertain the presence of polar charges in ZnO nanowires as the phenomenon leading to the formation of the switch. The disappearance of the resistive switching is also analyzed with two kinds of fabrication approaches Focused Ion/Electron Beam involved in the making the device and a summary of both length and fabrication dependences of resistive switching in the ZnO nanowire is presented. © *2013 AIP Publishing LLC*. [http://dx.doi.org/10.1063/1.4821994]

Conventional scaling methods have seen the dominance of certain tunable properties in functional materials like ZnO has given rise to a variety of applications.[1,2] Shrinking sizes also help realize higher memory densities, and higher computing performance.[3] Materials exhibiting twin resistive states have been used to demonstrate switching behaviour for data storage.[4] A host of interpretations are possible for a resistive switching device. Possible explanations derived from literature, associate itself with a variety of phenomena like electro-migration of oxygen ions,[5] filament formation,[6] charge trapping,[7] etc. Structurally a resistive switching device is fabricated from a simple model which is comprised of metal/oxide/metal. As a functional material, ZnO has been reported as a favorable material for switching in various morphologies.[6,8–10] Most reported ZnO nanowire based ReRAMs were fabricated using the conventional E-beam lithography through dissimilar metal workfunctions[8,11,12] and involved a multistep time intensive fabrication process. While there has been an effort to fabricate devices in this approach by a few groups in the past, little has been done to demonstrate a resistive switch, through simple fabrication techniques with similar metal workfunctions. We investigate a resistive switching device fabricated from an individual ZnO nanowire using Focused Electron Beam (FEB) and Focused Ion Beam (FIB) based direct write nanolithography techniques. The devices are fabricated with identical metal workfunctions (Pt) and analyzed for their interactions with the surrounding atmosphere. A detailed analysis of the DC Current-Voltage (I-V) curve is performed with respect to the mechanism of conduction. Our results present an approach to characterize the "resistive switch" in individual ZnO nanowires. Our interpretation of the observed resistive switching is elaborated on the basis of the existence of polar charges near the contacts and the I-V measurements data obtained at different partial pressures.

The ZnO nanowires were synthesized using CVD technique with ZnO and graphite powders as precursors.[13,14] For devices, the individual ZnO nanowires (6 devices) were subsequently connected to the pre-patterned electrodes using the electron beam induced deposition (EBID) of Platinum (Pt) metal-organic precursor ($(CH_3)_3CH_3C_5H_4Pt$) in FEI Quanta 200 3D dual beam system using the fabrication procedure reported elsewhere.[15] For ion beam induced deposition (IBID), a Ga ion beam of energy 30 keV with the beam current of 30 pA was used to decompose the same precursor resulting in the contact formation. The individual ZnO nanowire devices fabricated were subjected to Ar atmosphere-thermal annealing in a horizontal tube furnace system at 200 °C for 20 min. The microstructural characterization was performed using a 2100F JEOL Transmission electron microscope (TEM) at a voltage of 200 KeV. The sonicated solution of nanowires was drop casted on Cu grids for the preparation of TEM samples. All the electrical measurements of the ZnO nanowire devices were performed with a Keithley 4200-SCS parametric analyzer in a TTP-6 (Lakeshore Cryogenic, USA) probe station at ambient temperature in vacuum with the pressure ranging from 10^{-3} to 10^{-7} mbar.

Fig. 1(a) shows a bright-field TEM image of a ZnO nanowire used for the device fabrication, which was measured to have a thickness of around 150 nm. The perfect crystalline structure of the ZnO is demonstrated by its high-resolution TEM image (Fig. 1(b)). The FFT pattern (inset Fig. 1(b)) suggests that the ZnO nanowire was grown along [0 0 2] direction. Fig. 2(a) illustrates the I-V characteristics of an EBID fabricated individual ZnO nanowire device, with a channel length of 2.5 μm before and after Ar-annealing at 200 °C, in a single scan-sweeping mode. A scanning electron microscope image of the device is seen in the inset of Fig. 2(a). Before annealing, the device showed typical characteristic of a schottky contact between the EBID Pt and the ZnO nanowire (inset in Fig. 2(b)). After Ar-annealing, the current density was found to increase by 3 orders of

a)Email: yzhuang@ntu.edu.sg

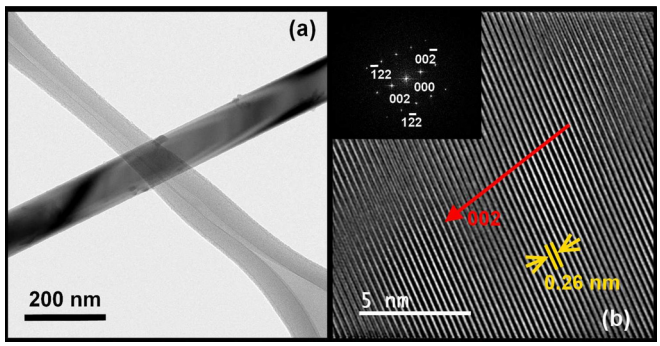

FIG. 1. (a) A Low magnification TEM image of a ZnO nanowire. (b) A HR-TEM of a ZnO nanowire with (002) as its growth direction. Inset: Indexed FFT pattern of the HR-TEM image.

magnitude. Fig. 2(b) presents the I-V curve in a dual scan-sweeping mode of a single ZnO nanowire device. The I-V characteristics of the annealed samples exhibit a small spike in the current at ~0.5 V during the forward scan and a dip at ~0.1 V during the reverse scan, forming a loop. Fig. 2(c) depicts the room temperature I-V characteristics of the annealed ZnO nanowire device, observed in a dual scan-sweeping mode from 0 V to 1.0 V measured at 10^{-7} mbar pressure. During the forward voltage sweep, the current takes an ohmic path from 0 V to 0.5 V, shifts from a high resistive state (HRS) to low resistive state (LRS) at 0.5 V (defined as the set voltage) and remains in this state up to 1.0 V. The reverse voltage sweep continues to be in LRS till 0.2 V (reset voltage) where it drops back to the HRS. The two resistive states can be controlled by the applied bias. The switching operation happens only once in the entire range of voltage scanned from −5 V to 5 V. The unipolar switching behaviour observed in our devices (six 2-3 μm EBID, two 5 μm EBID, two 2-3 μm IBID) is quite consistent with other nanowire devices.[9] Fig. 2(d) shows the variation of the resistive switching behaviour in the atmospheric pressure. The loop expands in area at high vacuum (10^{-7} mbar and 10^{-3} mbar) and gradually diminishes in atmospheric pressure. The inset in Fig. 2(d) presents two resistive states observed at 0.3 V at different atmospheric pressure implying a better on/off ratio (HRS/LRS) at 10^{-7} mbar as compared to the atmospheric pressure.

To reduce the schottly barrier resistance of the Pt-ZnO interface, the ZnO nanowire device was subjected to Ar-annealing at 200 °C. The TEM analysis of Yoon *et al.*[16] showed that annealing causes microstructural changes through sintering Pt nanoparticles with the reduction of carbon content in the deposited Pt and alloy formation, responsible for the enhancement of the conductivity of the device.[16] Our understanding is based on the assumption that the depletion width formed at the interface of the Schottky barrier between Pt and ZnO is altered in two possible ways: (i) annealing reduces the barrier height by thermally activating the hot electrons at the interface leading to an ohmic contact; (ii) IBID drastically alters the interface causing localised damage with a highly energetic beam of Ga ions.

The mechanism of switching can be explained on the basis of existence of polar surfaces, an idea derived from Song *et al.*[8] The existence of polar charges along the (0 0 1) basal planes gives ZnO the characteristic of a polar surface. Both ends of the basal plane in the nanowire are terminated with partially positive Zinc lattice sites and partially negative Oxygen lattice sites.[17] This gives rise to spontaneous polarization along the c-axis. Despite no surface reconstruction, the extraordinary stability of ZnO has given rise to a variety of nanostructures.[18] With favorable ohmic contacts between the Pt and ZnO, the electrons from Pt tend to migrate near the contact interface. At low voltages, some of the injected

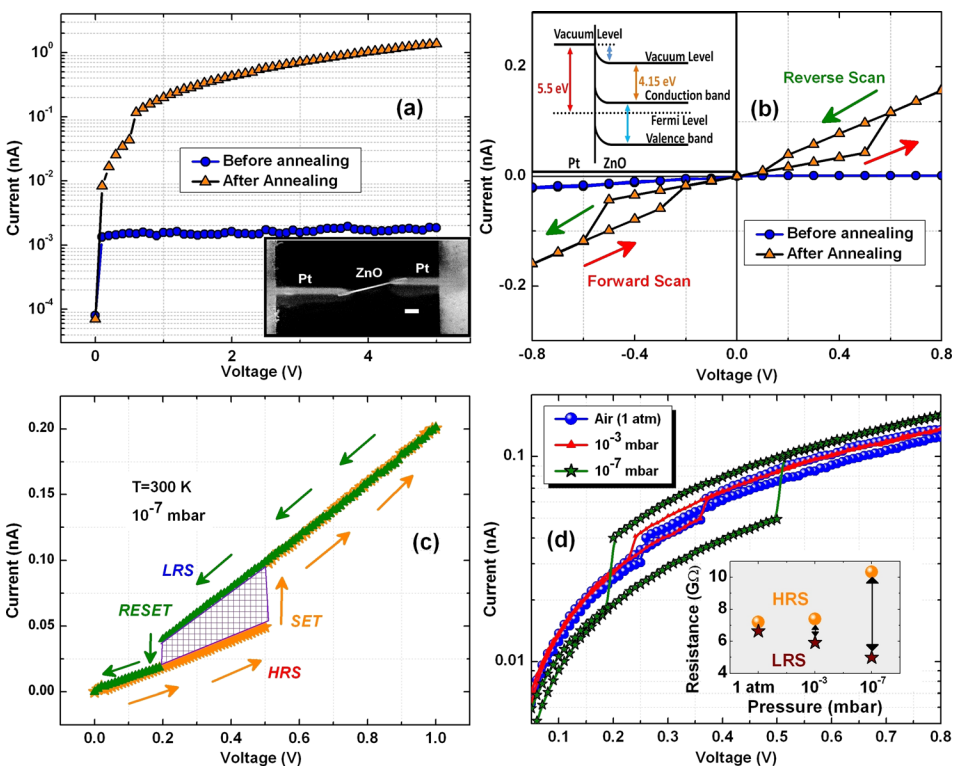

FIG. 2. (a) I-V characteristics of ZnO nanowire with Pt electrodes before and after annealing at 200 °C in Ar atmosphere. Inset: SEM image of Pt/ZnO nanowire/Pt device fabricated using FEB deposition. (b) A dual scan I-V characteristics of a Pt/ZnO nanowire/Pt device before and after Ar annealing. (c) A typical resistive switching of Pt/ZnO/Pt displaying HRS to LRS transition. (d) A log plot of the resistive switching of ZnO nanowire device at vacuum levels varying from 1 atm to 10^{-7} mbar. Inset: A plot of RS/LRS/ at respective vacuum pressures.

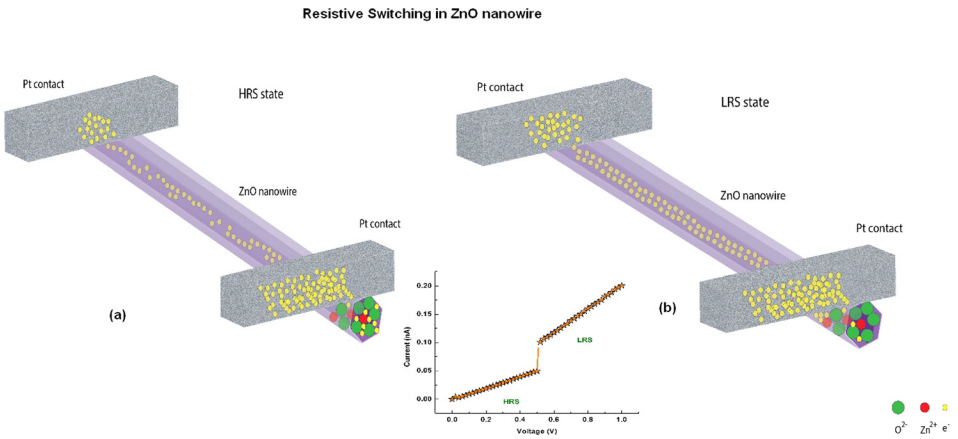

FIG. 3. A Schematic representation of the charges screened by the localized polar charges at the ends of the ZnO nanowire. (a) HRS state of the I-V curve (inset). (b) LRS state in the I-V curve.

electrons are trapped by the existing polar charges at the interface, observed as the HRS (Fig. 3(a)). Once the applied voltage increases beyond a point (Set voltage), the electrons are de-trapped from their polar charges, resulting in a spike in the current or the LRS state (Fig. 3(b)). Our experiments analyzing the pressure-dependent switching (Fig. 2(d)) support the hypothesis of polar charges behind the observed resistive switching. The atmospheric oxygen adsorbed on the surface neutralizes the polar charges, making the change in resistive states more negligible. It can be inferred from Fig. 2(d), as the test station is pumped down to higher vacuum, the concentration of surface adsorbents is decreased and the effect of the polar charges is more pronounced. The cyclic I-V curve (including the hysteresis loop) gives the power dissipated by the ZnO nanowire. We believe that the differences in the Set and Reset voltages are primarily due the joule heating in the nanowire. During the reverse scan, the joule heating in the ZnO nanowire provides up to 5 times more power at the set voltage point (~40 pW) as compared to power at the reset voltage point (~8 pW), which gives sufficient energy to escape the polar charge traps. This gives a dip in the reverse scan and a reset point (Fig. 2(c)).

The surface adsorbents not only alter the switching but also the conduction through the ZnO nanowire. It is the presence of such adsorbents on the nanowires surface that leads to a depletion region in the ZnO nanowire.[19] Classifying broadly, there are two kinds of trap sites observed in our ZnO nanowire device: (i) one at the interface where polar charges trap the charge carriers injected giving rise to switching, (ii) the second throughout the nanowire arising due to a variety of defects. For the latter in the ZnO nanowire, the transport after switching is dominated by the space charge limited current (SCLC), in which the electrons move through a spatial distribution of negative charges governed by trapping/detrapping kinetics.[14] The adherence to a power law not only confirms SCLC but also suggests the exponential distribution of traps between the conduction band and the Fermi level.[19] The trap limited mobility of the majority charge carrier was calculated to be 2.15×10^{-4} cm^2/Vs from the modified Child's law equation[20] $\mu_{SCLC} = (I/V^2)\ (8d/9\pi\varepsilon_0\varepsilon_r)$; where d (2.5 μm) is the channel length of the device. The number of charge carriers in the HRS state is given by

$$n_{HRS} = (R_{LRS}\, n_{LRS})/R_{HRS}. \quad (1)$$

R_{LRS} and R_{HRS} are obtained from Fig. 2(d) at 0.3 V and 10^{-7} mbar pressure. The calculations for $n_{LRS} = \sigma_{LRS}/e\mu_{SCLC}$ yield 1.85×10^{19} cm^{-3}. Subsequently, Eq. (1) gives the value for $n_{HRS} = 8.91 \times 10^{18}$ cm^{-3}.[14] From this, we observe that only a fraction of the charges get trapped near the interface due to the presence of the localized polar charges.

Fig. 4(a) depicts a typical switching process of a resistive switching device. The on/off ratio for the given reading voltage is about 1.5. The similarity between the current and

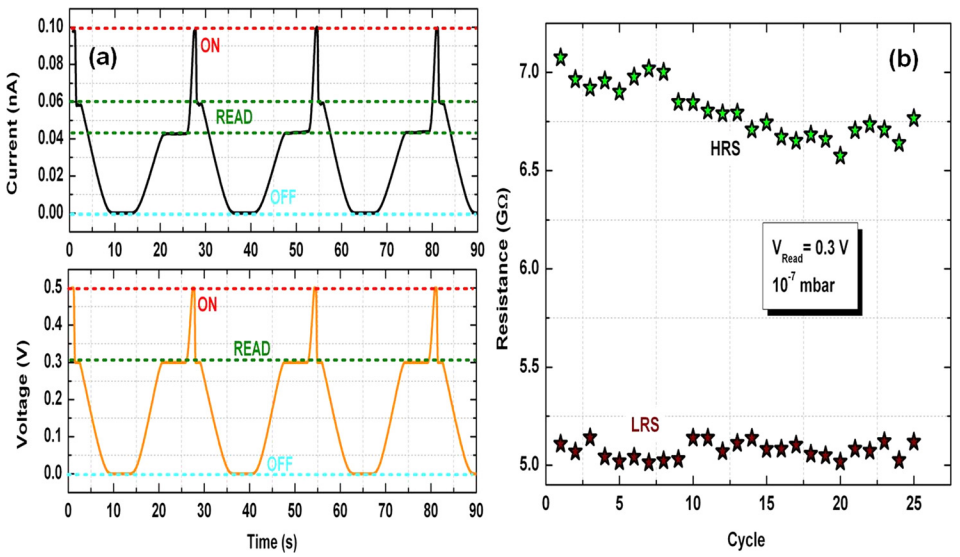

FIG. 4. (a) A programmable pulse voltage response displaying a ZnO nanowire device switching window with On/Off as 0.5 V/0 V and 0.3 V as reading voltage and corresponding current values traced by the device. (b) Stability test of a ZnO nanowire device for 25 cycles of operation at reading voltage.

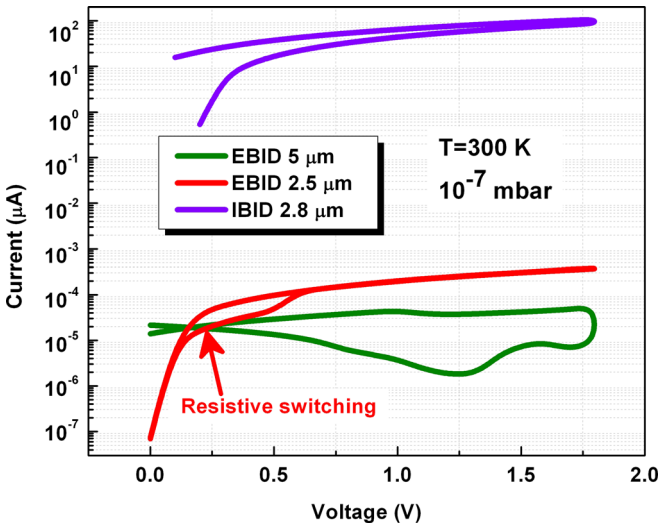

FIG. 5. Fabrication and channel length based comparative semi-log plot of the current-voltage curves of 2.5 μm, 5 μm EBID devices, and 2.8 μm IBID device. The switching is observed only in 2.5 μm EBID device.

voltage curves denotes perfectly reversible, stable, and non-destructive behaviour. Fig. 4(b) displays the stability of the resistive switch in a 25 cycle device operation. The currents in the nanowire retraced the same values after 25 cycles of operation.

The absence of resistive switching in the Pt/ZnO nanowire/Pt structure with the increase in channel length was observed (Fig. 5). A 5 μm device fabricated and annealed under the same conditions did not show any switching. This reinstates the explanations given by Song[8] that at a given voltage, the local electric field created due to the polar charges along the c-axis decreases and the loop vanishes. The total resistance of the structure (contacts + nanowire) now dominates over the screening effect of the polar charges. Additionally, fabrication techniques also affect the resistive switching due to polar charges. Although IBID performed using FIB's Ga ion beam results in low-resistive Ohmic contacts, it has always been associated with a variety of localized damages. IBID not only involves deposition, but also extensive sputtering of the surface of the nanowire being exposed under the ion beam.[21] The sputtering is accompanied by secondary phenomena such as surface amorphization/modification, doping of Ga ions and alloy formation.[21] Hence the exposure of nanowire under the ion beam could damage or neutralize the polar charges around the area where contacts are being fabricated. This might be one of the reasons why researchers reporting I-V characteristics of individual ZnO devices did not observe the switching.[22,23] From Fig. 5, we observed a similar scenario in our devices, where a 2.8 μm device fabricated/annealed using IBID failed to show switching characteristics despite high currents and low-resistive Ohmic contacts.

To summarize, we demonstrated a Pt/ZnO nanowire/Pt resistive switching device. The switching has been attributed to the presence of localized polar charges which create a local electric field along the c-axis of the nanowire. The enhancement in switching phenomenon was observed with the decrease in oxygen pressure. Pt-ZnO contacts in this case were evaluated and barrier modification through annealing was achieved. The role of traps contributing to the switching phenomena was studied. The role of longer channel lengths and destructive fabrication techniques, resulting in the absence of switching was evaluated. The switching in the ZnO nanowire device was observed to be stable and reversible. In addition to the growth of ZnO nanowires along the c-axis and shorter channel lengths, better fabrication techniques and practices should be involved to observe the effect of the polar charges. With ample of scope for improvement in fabrication procedures and reading window of the device, ZnO nanowires can be seen as one of the promising materials for the next-generation memories.

The authors wish to thank Dr. Nripan Mathews for his constructive suggestions for the manuscript and Hayden for his support in graphics.

[1]M. H. Huang, S. Mao, H. Feick, H. Yan, Y. Wu, H. Kind, E. Weber, R. Russo, and P. Yang, Science (New York, N.Y.) **292**, 1897–1899 (2001).
[2]Z. L. Wang and J. Song, Science (New York, N.Y.) **312**, 242–246 (2006).
[3]A. Sawa, Mater. Today **11**, 28–36 (2008).
[4]H. Y. Peng, G. P. Li, J. Y. Ye, Z. P. Wei, Z. Zhang, D. D. Wang, G. Z. Xing, and T. Wu, Appl. Phys. Lett. **96**, 192113 (2010).
[5]Y. Du, H. Pan, S. Wang, T. Wu, Y. P. Feng, J. Pan, and A. T. S. Wee, ACS Nano **6**, 2517–2523 (2012).
[6]A. Shih, W. Zhou, J. Qiu, H. J. Yang, S. Chen, Z. Mi, and I. Shih, Nanotechnology **21**, 125201 (2010).
[7]L. D. Bozano, B. W. Kean, V. R. Deline, J. R. Salem, and J. C. Scott, Appl. Phys. Lett. **84**, 607–609 (2004).
[8]J. Song, Y. Zhang, C. Xu, W. Wu, and Z. L. Wang, Nano Lett. **11**, 2829–2834 (2011).
[9]Y. D. Chiang, W. Y. Chang, and C. Y. Ho, IEEE Trans. Electron Devices **58**, 1735–1740 (2011).
[10]J. Qui, A. Shih, W. Zhou, Z. Mi, and I. Shih, J. Appl. Phys. **110**, 014513 (2011).
[11]D. Yeom, J. Kang, M. Lee, J. Jang, J. Yun, D.-Y. Jeong, C. Yoon, J. Koo, and S. Kim, Nanotechnology **19**, 395204 (2008).
[12]Y. Yang, X. Zhang, M. Gao, F. Zeng, W. Zhou, S. Xie, and F. Pan, Nanoscale **3**, 1917–1921 (2011).
[13]R. R. Prabhakar, N. Mathews, K. B. Jinesh, K. R. G. Karthik, S. S. Pramana, B. Varghese, C. H. Sow, and S. Mhaisalkar, J. Mater. Chem. **22**, 9678 (2012).
[14]See supplementary material at http://dx.doi.org/10.1063/1.4821994 for details about synthesis and charge trapping.
[15]K. R. G. Karthik, H. K. Mulmudi, K. B. Jinesh, N. Mathews, C. H. Sow, Y. Z. Huang, and S. G. Mhaisalkar, Appl. Phys. Lett. **99**, 132105 (2011).
[16]S. W. Yoon, J. H. Seo, K.-H. Kim, J.-P. Ahn, T.-Y. Seong, K. B. Lee, and H. Kwon, Thin Solid Films **517**, 4003–4006 (2009).
[17]S. Baruah and J. Dutta, Sci. Technol. Adv. Mater. **10**, 013001 (2009).
[18]Z. L. Wang, J. Phys.: Condens. Matter **16**, R829–R858 (2004).
[19]Z.-M. Liao, Z.-K. Lv, Y.-B. Zhou, J. Xu, J.-M. Zhang, and D.-P. Yu, Nanotechnology **19**, 335204 (2008).
[20]A. Talin, F. Léonard, B. Swartzentruber, X. Wang, and S. Hersee, Phys. Rev. Lett. **101**, 076802 (2008).
[21]A. Motayed, A. V. Davydov, M. D. Vaudin, I. Levin, J. Melngailis, and S. N. Mohammad, J. Appl. Phys. **100**, 024306 (2006).
[22]J. H. He, P. H. Chang, C. Y. Chen, and K. T. Tsai, Nanotechnology **20**, 135701 (2009).
[23]X.-B. He, T.-Z. Yang, J.-M. Cai, C.-D. Zhang, H.-M. Guo, D.-X. Shi, C.-M. Shen, and H.-J. Gao, Chin. Phys. B **17**, 3444–3447 (2008).